

Layer-by-layer-resolved quantum-well states in ultrathin silver islands on graphite: A photoemission study

F. Patthey and W.-D. Schneider

Institut de Physique Expérimentale, Université de Lausanne, CH-1015 Lausanne, Switzerland

(Received 22 August 1994)

Layer-resolved quantum-well states (QWS's) corresponding to islands of different thicknesses for ultrathin Ag films on graphite have been observed by angle-resolved ultraviolet photoemission. The spectral linewidth dependence on island thickness and on binding energy is well described within a phase-accumulation model, taking into account the specific quantum-well barriers involved. Thus high-resolution photoemission of QWS's provides an interesting tool to investigate the morphology and island-height distribution of ultrathin metal films.

The study of low-dimensional structures at the nanometer scale has attracted considerable interest since in such spatially confined systems electron-wave-vector quantization can be observed. This phenomenon is encountered in semiconductor quantum wells,¹ in two-dimensional metal overlayers,²⁻¹⁰ and recently, in quasi-zero-dimensional metallic quantum dots.¹¹ For example, in thin films grown epitaxially on substrates, periodic structure has been observed in electron-tunneling spectra representing a direct observation of size-dependent electronic states in thin metal films.² The spacing of the quantized energy levels is determined by the number of layers and provides a direct measurement of the electron group velocity while their location in energy determines the position of band edges and other critical energy states in the band structure of the metal.² Later on, such systems have been predicted to show fine oscillations also in their photoemission spectra caused by the quantization of hole states,¹² where the peaks are broadened only by the intrinsic lifetime of the hole state.¹² Valence level photoelectron spectroscopy and inverse photoemission of several metal-on-metal and metal-on-semiconductor overlayer systems essentially confirmed these predictions and have permitted the observation of quantum size effects.⁴⁻¹¹

However, electron-tunneling² and photoemission experiments¹¹ suffer from an inherent complication: in general they sample contributions from a range of island sizes or film thicknesses with a different number of layers that are superimposed according to their respective population. Therefore, in these studies, a distribution function had to be introduced to model the actual size or thickness distribution to obtain compatibility with the data. So far no direct experimental verification of such a size distribution for very thin films has been obtained.

In this work, we present direct observation of layer-by-layer-resolved island-thickness distributions of ultrathin Ag islands achieved by high-resolution photoemission of the quantum-well state (QWS). Moreover, we show quantitatively how this size distribution determines the linewidths as a function of binding energy and layer thickness and we deduce an upper limit for the QWS hole lifetime width (70 meV) which is compatible with theoret-

ical predictions of Loly and Pendry.¹² Thus high-resolution photoemission of QWS's provides an interesting tool to study the morphology and island-height distribution of ultrathin metal films.

The experiments were performed in an ultrahigh vacuum (UHV) photoemission chamber at a base pressure of less than 2×10^{-10} mbar. Photoelectrons were collected using a hemispherical electron analyzer (HA150 from VSW). The instrumental energy resolution was 50 meV and the angular resolution was $\pm 2^\circ$. Satellite-free photoelectron spectra were measured using the He I line (21.2 eV) of a high-intensity gas discharge lamp (GAMMADATA) combined with a custom built monochromator.¹³ The highly oriented pyrolytic graphite (HOPG) substrate was mounted on a cold finger held at 50 K by a closed cycle He refrigerator. A retractable electron gun allowed rapid heating of the substrate for cleaning and annealing. The HOPG crystal was cleaved in air before transfer into the vacuum chamber and then cleaned in UHV by a short heat flash (1200 K). After deposition of a given amount of silver layers at low temperature (50 K), the sample was annealed at room temperature for 1 min. At low temperature the growth mode of silver on HOPG is not determined unambiguously in spite of the discontinuous changes in the slope of the condensation curve ($4d$ -photoemission signal versus deposition time).¹⁴ At this stage the film is polycrystalline with a majority of crystallites exposing the Ag(111) surface as indicated in the photoemission valence-band spectrum. After annealing the spectrum is representative of a pure Ag(111) single crystal surface.¹⁵ Moreover, the contribution from the graphite substrate becomes visible in the photoemission spectrum showing that the film has transformed into islands with the Ag(111) orientation.

Figure 1 displays a typical spectrum of such a sample after annealing. The Ag $4d$ contribution between 4 and 7 eV binding energy is very intense compared to the weak sp band which appears as flat and structureless up to the Fermi level. An amplification of this part of the spectrum by a factor of 25 reveals fine oscillations which are the signature of the QWS (see, e.g., Ref. 7). In the present case the one-dimensional quantum-well barriers are formed by the Ag-vacuum and the Ag-graphite inter-

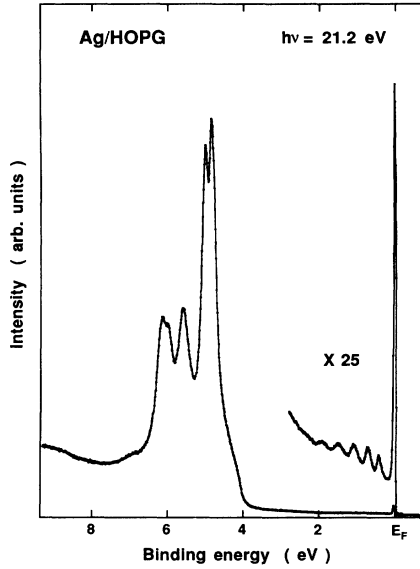


FIG. 1. Normal emission valence photoelectron spectrum of Ag(111) islands on graphite taken at 21.2-eV photon energy. The inset shows typical quantum-well-state oscillations just below the surface state at the Fermi level.

faces. In the energy range of interest, a gap in the band structure of graphite (see below) impedes the propagation of the electron wave function into the substrate. The intense structure at the Fermi level is easily identified as the well-known surface state of the (111) crystal face of silver.^{15,16} The sharpness of this surface state reflects the good crystallinity and orientation of the islands. In Fig. 2, a set of spectra in the range of the QWS (upper curves) is shown for six different samples. The thickness of the islands increases from the bottom to the top. The uppermost spectrum was recorded on a thick film (> 100 ML). It represents the bulk limit with the L edge of the Ag sp band at about 0.3 eV below the Fermi level. The other spectra were obtained on films with nominal thicknesses of 8, 14, 17, 28, with 32 ML. The following observations are made from Fig. 2: (i) the energy difference between successive QWS's diminishes with increasing film thickness, (ii) for a given film thickness the width of the QWS increases with binding energy, (iii) for a given binding energy the width of the QWS decreases with increasing film thickness, and (iv) the intensity of the QWS decreases with increasing film thickness.

In order to explain these observations we recall that for a one-dimensional quantum box the QWS energy E_n is given by¹⁷

$$2k(E_n)d + \phi(E_n) = 2\pi n, \quad (1)$$

where k is the electron wave-vector component perpendicular to the surface, $d = Na_0$ is the film thickness, where N is the number of layers and $a_0 = 2.36 \text{ \AA}$ is the distance between the layers, Φ is the total phase shift of the electron wave function from reflection at the Ag-vacuum and Ag-HOPG interfaces, and n is the quantum number enumerating the wells states. In Eq. (1), $k(E_n)$

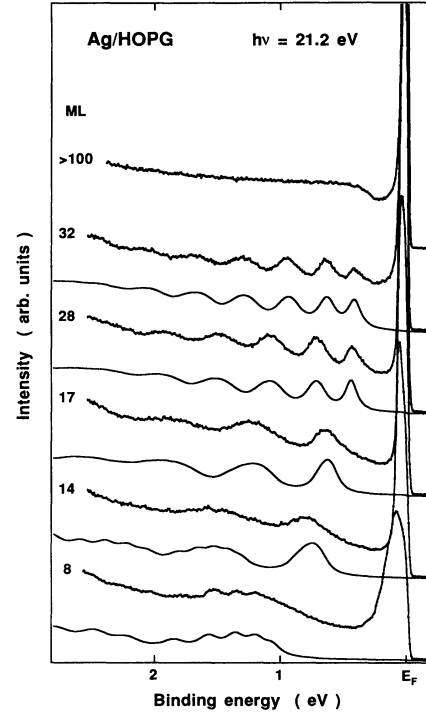


FIG. 2. Measured (as in Fig. 1) and calculated (continuous curves) photoemission spectra for the indicated coverages revealing the evolution of the quantum well states with island thickness. For the ultrathin Ag islands (8 ML) the new substructure is accounted for by the model calculation (see text) and monitors directly the island height distribution.

represents the band dispersion along the ΓL direction in the three-dimensional Brillouin zone of Ag, perpendicular to the Ag(111) surface. Thus observation (i) is obviously a consequence of Eq. (1). Observation (iv) is a consequence of the finite electron mean-free path leading to an exponential decrease of the photoemission signal.⁸ Observation (ii) could be explained by the lifetime dependence on binding energy¹⁸ but this is not consistent with observation (iii). The solution to the problem is contained in the spectrum at the bottom of Fig. 2 (8 ML) where the broad peak between 1 and 3 eV binding energy clearly displays the substructure. This important observation can be explained as follows: each substructure peak corresponds to a particular island thickness. The energy difference between each substructure peak is representative of a thickness difference of one monolayer of the island height. Thus the island thickness distribution is observed directly centered on the mean number of layers. It is this distribution that results in the broadening of the spectral linewidth as a function of binding energy and nominal film thickness.

In order to verify this hypothesis quantitatively a simple model is used to calculate the photoemission spectra. The dispersion relation $E(k)$ for Ag(111) in the Γ - L direction is simulated by the two band model

$$E(k) = E_0 - [ak^2 + U - (4abk^2 + U^2)^{1/2}], \quad (2)$$

with $a = \hbar^2/2m^*$ and $b = 3\pi^2/a_0^2$, where $U = 4.2$ eV is the width of the gap at the L symmetry point of Ag(111), $E_0 = 0.31$ eV is the position of the sp band edge relative to the Fermi level and $m^* = 0.7$ is the effective mass of the electrons in this band. The values of these parameters have been chosen in agreement with previous experiments.^{2,16,19,20} In the phase accumulation model¹⁷ the phase shift $\Phi(E)$ of the electron wave function in Eq. (1) is the sum of two terms: the shift at the outer quantum-well barrier at the Ag-vacuum interface

$$\Phi_B = \pi[3.4 \text{ eV}/(E_V - E)]^{1/2} - \pi, \quad (3)$$

which represents the phase shift for an image potential in the WKB approximation² and where E_V is the vacuum level. The second term is the phase shift at the inner quantum-well barrier at the Ag-graphite interface

$$\Phi_C = 2\arcsin[(E - E_L)/(E_U - E_L)]^{1/2}, \quad (4)$$

which is an empirical relation characteristic for a step potential.²² Here $E_L = -4$ eV and $E_U = 4$ eV are the positions of the lower and upper band gap at the Γ point in the $[111]$ direction of graphite,^{23,24} respectively. In order to model the photoemission spectra a Gaussian distribution of island thicknesses with a full width at half maximum of 2 ML is assumed. The width of each individual QW level is given by the hole lifetime convoluted with the instrumental energy resolution. Moreover, an integrated background due to inelastically scattered electrons was added to fit the experimental spectra. Since the mean island thickness is not known *a priori* (due to the island formation process by annealing) the layer thickness d is considered as a free parameter in the model calculation. It should be noted that the evolution of the Ag(111) surface state with film thickness (energy position, width, and intensity in Fig. 2) yields an independent indication of the actual number of layers involved,⁴ which is in agreement with the number of layers derived from the quantum-well model.

Figure 2 shows a comparison between the measured (upper curves) and calculated (lower thin curves) photoemission spectra for the different island thicknesses. The overall agreement between the data and model calculations is excellent. Even for the ultrathin islands (8 ML) shown at the bottom of Fig. 2 the fine structure in the data is satisfactorily reproduced by the calculation. Thus the simple one-dimensional quantum-well model which takes into account a realistic description of the band structure involved in combination with the phase accumulation model describes the essential physics of the problem. This is illustrated in Fig. 3 which shows the relationship between the Ag $E(k)$ dispersion along the Γ - L direction and the measured and calculated photoemission spectra for 8 and 28 ML. In the 28-ML spectrum shown in the top of Fig. 3, QWS's up to $n = 5$ can clearly be distinguished. Here the quantum state index n is counted from the top to the bottom of the band.² In the 8-ML spectrum shown in the bottom of Fig. 3, $n = 1$ QWS's from islands consisting of 7, 8, and 9 ML are clearly resolved individually thus elucidating the morphology of this thin film. The $n = 2$ QWS can also be observed start-

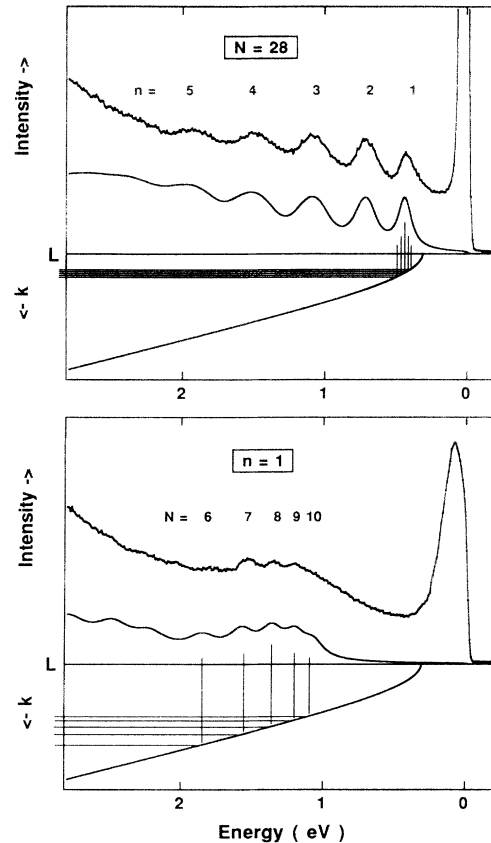


FIG. 3. Measured (as in Figs. 1 and 2) and calculated photoemission spectra of the quantum well states with the number of layers N and the quantum numbers n as indicated. In the lower part the relevant $E(k)$ dispersion is shown in order to illustrate the physical origin for the observation of the height distribution of the very thin islands (see text).

ing at binding energies > 2 eV. Why does the island-thickness distribution become experimentally visible only for the very thin islands? The answer is depicted graphically also in Fig. 3: For thin layers the k -value spacing becomes large [see Eq. (1)] leading to an expansion of the QWS from adjacent layers in a large energy interval. In addition, the influence of the band dispersion or group velocity on the energy spacing of the QWS is evident from Fig. 3. Moreover, due to the presence of the Ag L gap at 0.3 eV, the QWS cascades for all island thicknesses are "trapped" at this band edge and can never cross the Fermi level. When the QWS approaches the band edge, its spectral intensity diminishes (see Fig. 2 for 28 and 32 ML). This observation is in agreement with earlier findings and predictions,² and is due to the fact that at the band edge the group velocity approaches zero. The upper limit of the hole lifetime is essentially fixed by the width of the QWS in the bottom spectra of Figs. 2 and 3 and is found to be small compared to the apparent width of the levels in the spectra for larger thicknesses. Because of the shape of the dispersion curve $E(k)$ with a horizontal tangent at the L point, the bulk hole lifetime² can be deduced by extrapolation to $E = E_0$ for thick

films. Within the experimental uncertainty due to finite k resolution parallel to the surface an upper limit of 70 meV is obtained which is compatible with a theoretical prediction.¹² A slight increase of the QWS lifetime width (from 70 to about 100 meV) with binding energy is observed in the bottom spectra of Figs. 2 and 3. This effect may be due to the fact that the hole states are not completely trapped in the thin islands but can escape to the substrate.¹²

To summarize, a series of QWS's in thin Ag islands deposited on HOPG is observed by angle-resolved high-resolution ultraviolet photoemission. For ultrathin islands of less than ten atomic layers a new observation is made; the spectrum of the low quantum number QWS

clearly displays several substructure peaks. An analysis of these new spectral features within a phase accumulation model taking account of the specific quantum-well barriers involved shows that each substructure peak represents a QWS originating from islands of a given thickness. Thus for very thin metal islands photoelectron spectroscopy is able to monitor the island morphology via the QWS with atomic layer depth resolution.

It is a pleasure to thank R. Berndt, E. Bullock, and B. Delley for stimulating discussions. The financial support from the Swiss National Science Foundation is gratefully acknowledged.

¹L. L. Chang, in *Highlights in Condensed Matter Physics and Future Prospects*, edited by L. Esaki (Plenum, New York, 1991), p. 83.

²R. C. Jaklevic and J. Lambe, *Phys. Rev. B* **12**, 4146 (1975).

³C. Marlière, *Vacuum* **41**, 1192 (1990).

⁴A. L. Wachs, A. P. Shapiro, T. C. Hsieh, and T. C. Chiang, *Phys. Rev. B* **33**, 1460 (1986).

⁵S. A. Lindgren and L. Wallden, *Phys. Rev. Lett.* **59**, 3003 (1987); **61**, 2894 (1988).

⁶T. Miller, A. Samsavar, G. E. Franklin, and T. C. Chiang, *Phys. Rev. Lett.* **61**, 1404 (1988).

⁷M. A. Mueller, A. Samsavar, T. Miller, and T. C. Chiang, *Phys. Rev. B* **40**, 5845 (1989); M. A. Mueller, T. Miller, and T. C. Chiang, *ibid.* **41**, 5214 (1990).

⁸M. Jalochoowski, H. Knoppe, G. Lilienkamp, and E. Bauer, *Phys. Rev. B* **46**, 4693 (1992).

⁹F. J. Himpsel, *Phys. Rev. B* **44**, 5966 (1991).

¹⁰J. E. Ortega and F. J. Himpsel, *Phys. Rev. Lett.* **69**, 844 (1992).

¹¹D. A. Evans, M. Alonso, R. Cimino, and K. Horn, *Phys. Rev. Lett.* **70**, 3483 (1993).

¹²P. D. Loly and J. B. Pendry, *J. Phys. C* **16**, 423 (1983).

¹³H.-V. Roy, J. Boschung, F. Patthey, P. Fayet, W.-D. Schneider, and B. Delley, *Phys. Rev. Lett.* **70**, 2653 (1993).

¹⁴G. Polanski and J. P. Toennies, *Surf. Sci.* **260**, 250 (1992).

¹⁵P. Heimann, H. Neddermeyer, and H. F. Roloff, *J. Phys. C* **10**, L17 (1977).

¹⁶R. Wern, B. Courths, G. Leschik, and S. Hüfner, *Z. Phys. B* **60**, 293 (1985).

¹⁷N. V. Smith, N. B. Brookes, Y. Chang, and P. D. Johnson, *Phys. Rev. B* **49**, 332 (1994).

¹⁸J. B. Pendry, in *Photoemission and the Electronic Properties of Surfaces*, edited by B. Feuerbacher, B. Fitton, and B. R. Willis (Wiley, New York, 1978).

¹⁹L. Wallden and T. G. Gustafsson, *Phys. Scr.* **6**, 73 (1972).

²⁰B. Reihl and R. R. Schlittler, *Phys. Rev. B* **29**, 2267 (1984).

²¹N. V. Smith, *Phys. Rev. B* **32**, 3549 (1985).

²²P. M. Echenique and J. B. Pendry, *Prog. Surf. Sci.* **32**, 111 (1989).

²³D. Marchand, C. Frétigny, M. Laguës, F. Batallan, Ch. Simon, I. Rosenman, and R. Pinchaux, *Phys. Rev. B* **30**, 4788 (1984).

²⁴Th. Fauster, F. J. Himpsel, J. E. Fischer, and E. W. Plummer, *Phys. Rev. Lett.* **51**, 430 (1983).